Comitato Nazionale per L'Energia Nucleare
ISTITUTO NAZIONALE DI FISICA NUCLEARE

Sezione Siciliana
Gruppo di Catania
63/1

INFN/BE-63/1
22 Aprile 1963

A. Agodi, R. Giordano and G. Schiffrer:
ANALYSIS OF DIRECT (n, p) REACTIONS.

Reparto Tipografico
dei Laboratori Nazionali di Frascati
Cas. Postale 70 - Frascati (Roma)

Istituto Nazionale di Fisica Nucleare
Sezione Siciliana - Gruppo di Catania

INFN/BE-63/1
22 Aprile 1963

A. Agodi, R. Giordano and G. Schiffrer: ANALYSIS OF DIRECT (n, p) REACTIONS. (+)

ABSTRACT.

A simple picture is given for direct (n, p) reactions, based on the distorted wave Born approximation and on a single-particle model of the target and residual nuclei. Several angular distribution curves have been calculated in the zero-range approximation for the reaction $^{28}Si(n, p)^{28}Al$, induced by 14 MeV neutrons and leading to the ground state and to the first excited state of the residual nucleus. We have shown that, in our case, these two transitions give rise to the same angular distribution and the cross sections are in the ratio $\sigma_1/\sigma_2 = (2J_1 + 1)/(2J_2 + 1)$, where J_1 and J_2 are the total angular momenta of the two states.

The agreement with the experimental data turns out to be rather poor for any reasonable choice of the optical model and bound states parameters.

We have shown that the striking difference between the Born approximation and the distorted wave Born approximation curves can be explained in terms of a definite change in the relation between linear and angular momentum transfer.

(+) - This work has been supported in part by INFN, CRRN, CISE and CSFN.

1 - INTRODUCTION.

In the last few years much work has been carried out on direct nuclear reactions[1, 2], mainly in the distorted wave Born approximation, in order to get an understanding of both nuclear structure and reaction mechanism. However, most of the calculations have been performed for inelastic scattering and stripping (or pick-up) reactions.

We point out that the reactions involving different nucleons in the initial and in the final channels are, in certain respects, simpler to treat. In fact, in this case it is easier to take into account the antisymmetry of the wave functions[3]; one can also avoid the complications due to the optical model scattering from excited nuclei and to the description of the excited state itself. On the other hand, calculations without the restriction of the zero-range interaction are rather difficult when deuterons or α particles are involved.

The aim of this paper is to present an analysis of (n, p) reactions in the distorted wave Born approximation and the theoretical framework is designed to include a finite range neutron-proton interaction with exchange effects. In sec. 2 we give an account of this framework and for convenience we first treat the case of spinless particles and then introduce the spins. In sec. 3 we investigate the particular case of the reaction ^{28}Si(n, p)^{28} Al.

This reaction has been chosen due to the existence of experimental data[4] for the transitions leading to the ground state and to some low lying excited states of the residual nucleus; furthermore, in the nucleus ^{28}Si the state $1d_{5/2}$ is completely filled with neutrons and protons, what simplifies the shell model description. Unfortunately, this nucleus is not expected to be spherical, owing to the large positive quadrupole moments of nuclei[5] with mass number $20 \leq A \leq 30$. On the other hand, heavier nuclei like ^{40}Ca, which is certainly spherical, do not show any evidence of structures in the high energy proton spectrum[6].

The disagreement of the theoretical curves with the experimental one, which persists for any reasonable variation in the available parameters, does not allow us to draw very definite conclusions from the comparison of our calculations with the observed angular distribution. Nevertheless, we think that our results are of some interest in giving a new insight into the relation between the Born approximation and the distorted wave Born approximation with zero-range effective interaction, in the case of (n, p) reactions.

In particular, we have found that the optical model selection of important angular momenta in the initial and the final channel is sufficient to explain qualitatively the distorsion effects in the angular distribution.

2 - THE THEORETICAL SCHEME.

2. 1 - Basic assumptions.

The main assumptions underlying our treatment of (n, p) reactions can be summarized in the following statements.

The reaction is described as a single step transition from the initial to the final optical model scattering states, i. e. according to the distorted wave Born approximation[3, 7, 8, 9, 10].

We can neglect the interaction of the incident neutron with all nucleons, except with the least bound proton, since we are considering only transitions to states of low excitation energy. The effect of the Pauli principle can also be neglected, provided we are only interested in the shape of the angular distribution and not in the absolute value of the cross section. In fact, the antisymmetrization of the wave functions changes the differential cross section only by a constant factor[3].

The initial states of a bound nucleon are classified by the radial quantum number n, the orbital angular momentum k, the total angular momentum j and its projection γ. The final states are labelled by the corresponding primed quantum numbers.

The target is a closed shell nucleus both for neutrons and for protons. Therefore the residual nucleus has a proton hole and an extra-shell neutron.

The interaction which causes the transition is given by a neutron-proton central potential, containing a Wigner and a Majorana term.

2. 2 - Spinless particles.

On the basis of the assumptions of section 2. 1, we give here explicit expressions for the transition amplitude and for the differential cross section; the spins of the three particles involved in the reaction (neutron, proton and nuclear core) are not taken into account in this section.

The differential cross section can be expressed in terms of a transition amplitude $R_{\kappa\kappa'}$ which can be written as

$$(1) \qquad R_{\kappa\kappa'} = \int \psi^{(-)*}(\vec{r}_p)\, w^{*}_{n'k'\kappa'}(\vec{r}_n)\, \mathcal{U}\, \varphi^{(+)}(\vec{r}_n)\, v_{nk\kappa}(\vec{r}_p)\, d\tau,$$

where $d\tau$ indicates a six dimensional integration over the neutron and proton coordinates $\vec{r}_n$ and $\vec{r}_p$. The operator $\mathcal{U}$, denoting the neutron--proton potential, is given by

$$\mathcal{U} = (\alpha + \beta)^{-1} U(|\vec{r}_n - \vec{r}_p|)\,(\alpha + \beta P_x), \tag{2}$$

where P_x is the Majorana operator and α and β are real numbers.

The bound states for the neutron and the proton are represented by the normalized wave functions:

$$w_{n'k'\kappa'}(\vec{r}_n) = W_{n'k'}(r_n)\, Y_{k'\kappa'}(\vartheta_n, \varphi_n) \tag{3a}$$

$$v_{nk\kappa}(\vec{r}_p) = v_{nk}(r_p)\, Y_{k\kappa'}(\vartheta_p, \varphi_p); \tag{3b}$$

the indices κ and κ' are the projections of the orbital angular momenta k and k' respectively. As usually, $Y_{a\alpha}(\vartheta, \varphi)$ denotes the normalized spherical harmonic function[11]. The quantities $\psi^{(+)}(\vec{r}_n)$ and $\psi^{(-)}(\vec{r}_p)$ in eq. (1) are the optical model[12] scattering wave functions for neutrons and protons; the first has asymptotic boundary conditions of outgoing waves, the second of incoming waves. They may be expanded in the following form, when the optical potential is spherically symmetric[13]:

$$\psi^{(+)}(\vec{r}) = \sum_{l=0}^{\infty} \left[4\pi(2l+1)\right]^{1/2} i^l f_l(r) Y_{l0}(\vartheta) \tag{4a}$$

$$\psi^{(-)}(\vec{r}) = 4\pi \sum_{l=0}^{\infty} \sum_{\lambda=-l}^{+l} i^l g_l^*(r) Y_{l\lambda}^*(\Theta, \Phi) Y_{l\lambda}(\vartheta, \varphi). \tag{4b}$$

The functions $f_l(r)$ and $g_l(r)$ are solutions of the radial Schroedinger equation and are defined by the boundary conditions

$$\lim_{r\to 0} r\, f_l(r) = 0$$

$$\lim_{r\to\infty} f_l(r) = e^{i\delta_{nl}} (k_n r)^{-1} \sin\left(k_n r - \frac{1}{2} l\pi + \delta_{nl}\right)$$

$$\lim_{r\to 0} r\, g_l(r) = 0$$

$$\lim_{r\to\infty} g_l(r) = e^{i(\delta_{pl} + \sigma_l)} (k_p r)^{-1} \sin\left(k_p r - \frac{1}{2} l\pi + \eta \log 2k_p r + \delta_{pl} + \sigma_l\right);$$

the complex quantities δ_{nl} and δ_{pl} represent the optical model phase shifts for neutron and protons; the real quantity σ_l is the Coulomb

phase shift [14], given in terms of the Coulomb parameter [14] η by the definition $\sigma_l = \arg\Gamma(l+1+i\eta)$. We have chosen the polar axis in the direction of the momentum $\hbar\vec{k}_n$ of the incident neutron. The angles Θ and Φ give the direction of the momentum $\hbar\vec{k}_p$ of the emitted proton.

We have expressed the amplitude (1) by using the expansion of the potential $U(|\vec{r}_n - \vec{r}_p|)$ in terms of Legendre polynomials

$$U(|\vec{r}_n - \vec{r}_p|) = \sum_{L=0}^{\infty} U_L(r_n, r_p)\, P_L\left(\frac{\vec{r}_n \cdot \vec{r}_p}{r_n\, r_p}\right). \tag{5}$$

Then, after substitution of eqs. (2), (3), (4) and (5) into eq. (1), we can express the angular integrals in terms of vector addition coefficients as follows [11]:

$$\int Y^*_{c\gamma}(\Omega) Y_{b\beta}(\Omega) Y_{a\alpha}(\Omega)\, d\Omega = \left[\frac{(2a+1)(2b+1)}{4\pi(2c+1)}\right]^{1/2} \cdot (ab|c)(ab\alpha\beta|c\gamma). \tag{6}$$

For the vector addition coefficients we use the definition of ref. [15] and the notation $(ab\alpha\beta\,|\,abc\gamma) = (ab\alpha\beta|c\gamma)$; $(aboo|abco) = (ab|c)$. The expression for the transition amplitude $R_{\kappa\kappa'}$ is obtained from eqs. (1), (2), (3), (4), (5), and (6); it is

$$R_{\kappa\kappa'} = R^{(D)}_{\kappa\kappa'} + R^{(E)}_{\kappa\kappa'} \tag{7}$$

$$R^{(D)}_{\kappa\kappa'} = \frac{\alpha}{\alpha+\beta}(4\pi)^{3/2} \sum_{ll'L} (-)^{x'} i^{l-l'} (2l+1)\left[\frac{2k+1}{(2k'+1)(2l'+1)}\right]^{1/2} \cdot (1L|k')(kL|l') \cdot (1L0\kappa'|k'\kappa')(kL\,\kappa-\kappa'/l'\kappa-\kappa')\, I_{ll'L}\, Y_{l'\kappa-\kappa'}(\Theta,\Phi). \tag{8}$$

$$R^{(E)}_{\kappa\kappa'} = \frac{\beta}{\alpha+\beta}(4\pi)^{3/2} \sum_{ll'L} (-)^{\kappa-\kappa'} i^{l-l'} (2l+1)\left[\frac{2k+1}{(2k'+1)(2l'+1)}\right]^{1/2} \cdot (kL|k')(lL|l') \cdot (kL\kappa, \kappa'-\kappa/k'\kappa')(1L0\kappa-\kappa'/l'\kappa-\kappa')\, K_{ll'L}\, Y_{l'\kappa-\kappa'}(\theta,\phi). \tag{9}$$

The quantities $I_{ll'L}$ and $K_{ll'L}$ are radial integrals defined as

$$I_{ll'L} = \int_0^\infty\int_0^\infty g_{l'}(r_p)\, w_{n'k'}(r_n)\, U_L(r_n, r_p) f_l(r_n) v_{nk}(r_p) r_n^2 r_p^2 dr_n dr_p \tag{10a}$$

$$(10b)\quad K_{ll'L} = \iint_{0}^{\infty} g_{l'}(r_n)\, w_{n'k'}(r_p) U_L(r_n, r_p) f_l(r_n) v_{nk}(r_p) r_n^2 r_p^2 dr_n dr_p \,.$$

The resulting differential cross section is given by

$$(11)\quad \frac{d\sigma_0}{d\Omega} = \frac{1}{2k+1} \frac{M_n M_p}{(2\pi\hbar^2)^2} \frac{k_p}{k_n} \sum_{\kappa\kappa'} \left| R_{\kappa\kappa'} \right|^2$$

where M_n and M_p are the reduced masses in the initial and in the final channel.

In the case of a pure Wigner force, the parameter β in eqs. (8) and (9) vanishes, and the cross section (11) reduces to

$$\frac{d\sigma_0}{d\Omega} = \left(\frac{2M}{\hbar^2}\right)^2 \frac{k_p}{k_n} \sum i^m (2l+1)(2p+1) \left[(2l'+1)(2p'+1)\right]^{1/2} \cdot$$

$$(12)\quad \cdot (lL/k')(pP/k') \cdot (kL/l')(kP/p')(lp/n)(l'p'/n) \cdot W(lLpP;k'n) \cdot$$

$$\cdot W(l'Lp'P;kn) \cdot I_{ll'L} I^*_{pp'P} P_n(\cos\theta),$$

where the summation Σ is extended over the indices l, l', p, p', L, P and n; $m = l + l' + p + p'$ and $M = (M_n M_p)^{1/2}$. This expression can be obtained from eqs. (7), (8) and (11) using a well known property of spherical harmonics[11] and the sum rule of Racah[11, 16]. The quantities $W(a, b, c, d; ef)$ are defined as in refs. [11, 16].

In the particular case $k' = 0$ (which is of interest for the reaction $^{28}Si(n, p)^{28}Al$), the matrix element given by eqs. (7), (8), and (9) simplifies to

$$R_{\kappa 0} = (4\pi)^{3/2} \sum_{ll'} i^{l-l'} \left(\frac{2k+1}{2l'+1}\right)^{1/2} (lk/l')(lk0\kappa/l'\kappa) \cdot$$

$$\cdot F_{ll'} Y_{l'\kappa}(\theta, \phi) \qquad (k' = 0).$$

with the definition

$$F_{ll'} = (\alpha+\beta)^{-1} \left(\alpha I_{ll'l} + \beta \frac{2l+1}{2k+1} K_{ll'k}\right).$$

We note that in this case the direct and the exchange integrals have a

common geometrical factor. The cross section takes the form

$$\frac{d\sigma_o}{d\Omega} = \left(\frac{2M}{\hbar^2}\right)^2 \frac{k_p}{k_n} (-)^k \sum i^q \left[(2l'+1)(2p'+1)\right]^{1/2} (lk/l'0)\cdot$$

$$\cdot (pk/p'0)(lp/n0)(l'p'/n0)\cdot W(ll'pp'; kn)\, F_{ll'} F^*_{pp'} P_n(\cos\theta), \tag{13}$$

$$(k' = 0)$$

where the summation Σ is extended over the indices l, l', p, p', n, and $q = l - l' - p + p'$.

2. 3 - Particles with spin.

We now introduce the spin of the particles. Let σ be the projection of the proton spin on the Z axis and χ_σ the corresponding eigenfunction. Then, according to section 2. 1, we can write the proton bound state wave function as

$$v_{nkj\gamma}(\vec{r}_p) = v_{nk}(r_p) \sum_{k\sigma} \left(k\,\tfrac{1}{2}\,k\sigma/j\gamma\right) Y_{kk}(\vartheta_p, \varphi_p)\, \chi_\sigma$$

and a similar expression for the neutron wave function $w_{n'k'j'\gamma'}(\vec{r}_n)$. The spins of the unbound particles are left uncoupled.

The transition amplitude $R_{\sigma\sigma'\Gamma\Gamma'}$ from a state (J, Γ) of the target nucleus, characterized by the total angular momentum J and its projection Γ, to a state (J', Γ') of the residual nucleus, can be expressed in terms of the amplitude (7). If the core is in an angular momentum state $(j_o\gamma_o)$ we have

$$R_{\sigma\sigma'\Gamma\Gamma'} = \sum_{\substack{kk' \\ \gamma\gamma'\gamma_o}} \left(k\,\tfrac{1}{2}\,k\sigma/j\gamma\right)\left(k'\,\tfrac{1}{2}\,k'\sigma'/j'\gamma'\right)\left(jj_o\gamma\gamma_o/J\Gamma\right)\cdot$$

$$\cdot \left(j'j_o\gamma'\gamma_o/J'\Gamma'\right) R_{kk'}. \tag{14}$$

The cross section is then

$$\frac{d\sigma_{jj'}}{d\Omega} = \frac{1}{2(2J+1)} \left(\frac{M}{2\pi\hbar^2}\right)^2 \frac{k_p}{k_n} \sum_{\sigma\sigma'\Gamma\Gamma'} \left| R_{\sigma\sigma'\Gamma\Gamma'} \right|^2. \tag{15}$$

Of course, the angular distribution given by eq. (15) is different in gene

ral from that given by eq. (11), because the sum over κ and κ' is made in eq. (11) after squaring the amplitude and in eq. (15) before doing this. Nevertheless the two angular distributions are equal when $R_{\kappa\kappa'}$ does not depend on σ or σ' and at least one of the quantum number j_o, k, k' vanishes. This can be seen from eq. (14), using the orthogonality of the vector addition coefficients. In the case k'=0 we have

$$\sum_{\sigma\sigma'\Gamma\Gamma'} \left| R_{\sigma\sigma'\Gamma\Gamma'} \right|^2 = \frac{(2J'+1)(2J+1)}{(2k+1)(2j_o+1)} \sum_{\kappa}' \left| R_{\kappa o} \right|^2 \tag{16}$$

$(k' = 0).$

According to eqs. (11), (15) and (16), the cross section $d\sigma_{JJ'}/d\Omega$ is therefore proportional to $d\sigma_o/d\Omega$. One finds

$$\frac{d\sigma_{JJ'}}{d\Omega} = \frac{2J' + 1}{2(2j_o+1)} \cdot \frac{d\sigma_o}{d\Omega} , \qquad (k'=0) \cdot \tag{17}$$

In the other two cases we get

$$\frac{d\sigma_{JJ'}}{d\Omega} = \frac{2J' + 1}{2(2k'+1)} \cdot \frac{d\sigma_o}{d\Omega} , \qquad (j_o=0)$$

$$\frac{d\sigma_{JJ'}}{d\Omega} = \frac{2J'+1}{2(2k'+1)(2j_o+1)} \frac{d\sigma_o}{d\Omega} , \quad (k=0) \cdot$$

One should note that in the general case, if we sum over all values of J', such that $|j'-j_o| \leq J' \leq j'+j_o$, we get the same result as in the case $j_o = 0$. This can also be easily derived from eqs. (14) and (15), using the orthogonality property of the vector addition coefficients

$$\sum_{J'\Gamma'} (j'j_o\gamma'\gamma_o/J'\Gamma')(j'j_o\varepsilon'\varepsilon_o/J'\Gamma') = \delta_{\gamma'\varepsilon'}\,\delta_{\gamma_o\varepsilon_o} \cdot \tag{18}$$

3 - THE REACTION $^{28}Si(n, p)^{28}Al$.

3. 1 - General considerations.

Let us consider now the reaction $^{28}Si(n, p)^{28}Al$, at 14. 1 MeV neutron energy in the laboratory system. We have calculated the angular distribution of the protons emitted in the transitions to the ground state and to the first excited state of the nucleus ^{28}Al. In the previously discussed scheme, this angular distribution is given by eq. (13).

In the nucleus ^{28}Si we have 14 neutrons and 14 protons filling all states up to the $1d_{5/2}$-shell. In the nucleus ^{28}Al a proton is missing from this shell and a neutron is added in the $2s_{1/2}$-shell. For this reason the ground state of ^{28}Al splits actually into two states, with angular momenta $J_1=3$ and $J_2=2$. In fig. 1 is shown the level scheme of the nucleus ^{28}Al (ref. [17]). According to eq. (17) the two transitions give rise to the same angular distribution for protons and the integrated cross sections are in the ratio $\sigma_1/\sigma_2 = (2J_1+1)/(2J_2+1) = 7/5$. It is important to point out that this result depends neither on the particular choice of the optical model parameters, nor on particular assumptions about the neutron-proton force, provided that the amplitude $R_{kk'}$ does not depend on the spin projections σ or σ'. It depends indeed on our picture of the bound states and on the fact that $k' = 0$. It is also peculiar of (n, p) (or (p, n)) reactions; in inelastic scattering two such levels would give different angular distributions[18] for $k' = 0$. In the case of a non-spherical core, k' is no longer a good quantum number and again this property would not be valid.

These considerations suggest that a comparison with experiments of the angular distributions given by the two levels separately could give some informations about the validity of our model. Unfortunately, the splitting of the two levels amounts to 31 KeV only (see fig. 1) and the experimental angular distribution[4] is due to the unresolved levels. In the case of unresolved levels we can also use eqs. (7), (8), (9) and (11) instead of eqs. (14) and (16), owing to the sum rule (18).

3. 2 - Numerical calculations.

A detailed account of the methods employed for the numerical calculations is given in ref. [19]. We have studied a computer program for a delta-function neutron-proton potential, normalized as a Yukawa interaction of strength U_o and range μ^{-1}

$$(19) \qquad \mathcal{U} = 4\pi U_o \mu^{-3} \delta(\vec{r}_n - \vec{r}_p),$$

and for a potential as given in eq. (2), with a Yukawa radial shape. In the present paper we discuss only results obtained with the zero-range

potential (19). For the bound particles we have used isotropic harmonic oscillator wave functions[20], which are

$$v_{12}(r_p) = \left[\frac{16\,\lambda_p^{7/2}}{15\sqrt{\pi}} \right]^{1/2} \exp\left[-\frac{\lambda_p}{2} r_p^2 \right] r_p^2$$

$$w_{20}(r_n) = \left[\frac{6\,\lambda_n^{3/2}}{\sqrt{\pi}} \right]^{1/2} \exp\left[-\frac{\lambda_n}{2} r_n^2 \right] \left(1 - \frac{2}{3}\,\lambda_n r_n^2\right) .$$

The turning point R_o of the corresponding classical oscillator is related to the parameter λ_x by $R_{ox} = (7/\lambda_x)^{1/2}$ (x = n for neutron, x = p for proton). The optical model scattering solutions have been computed using a Saxon-Woods central potential well

$$\mathcal{V}_x(r) = -(V_x + iW_x) \left[\exp\left(\frac{r - R_x}{a_x}\right) + 1 \right]^{-1} .$$

Coulomb effects for protons have been taken into account exactly, assuming a uniform charge distribution of radius R_p for the residual nucleus ^{28}Al.

3.3 - Results.

The numerical calculations have been performed for several sets of input parameters, with the aim of clarifying the dependence of the theoretical curves on these parameters. Other curves have been calculated by suitably selecting the angular momenta in both the initial and the final channel, in order to get some insight into the relation between angular momentum and linear momentum transfer effects.

The curves plotted in figs. 2 to 6 are reported as examples to show the parameter dependence. They have been numbered according to table 1. The figs. 2 to 4 display the essential stability of the calculated pattern against changes in the radial extension of the bound state wave functions as well as in the optical potentials. The latter have been changed here only slightly with respect to those determined from elastic scattering[21, 22], since otherwise the very meaning of the theory would be altered. The effects of large variations in the optical potentials are shown in figs. 5 and 6. We give in fig. 5 an example of how the curves change when the real parts of the optical potentials are decreased by 25% with respect to the elastic scattering values. In fig. 6 the distorted wa-

ve curve is compared with those obtained without distortions and with Coulomb distortion only.

Though not improving the agreement with the experimental points, the effect of the optical model distortions appears to be quite important. This was expected on the basis of the evidence from inelastic scattering calculations[1] and from recent work on (p, n) reactions[23]. This situation qualitatively differs from the one we are faced with in the case of stripping[24], where the angle corresponding to the first forward maximum in the angular distribution is essentially unchanged by distortion effects. The position of this maximum is determined in a well known way[25] by a relation between the linear and the angular momentum transfers, which therefore seems to remain meaningful with and without distortions. In the case of (n, p) reactions the maximum of the Born approximation angular distribution can be determined by an analogous relation, as in the case of stripping, but it follows from the different behaviour of curves N. 2 and N. 11 (see fig. 6) that the effect of distortion is to change the relation between the linear and the angular momentum transfers.

We can observe that not all the matrix elements $F_{ll'}$ in eq. (13) have the same importance in the angular distribution; apart from resonance effects, the overlap of the wave functions is mainly responsible of the smallness of the contribution from certain states of angular momenta l and l'. In the zero-range approximation this can be estimated very simply: since the product of the two bound state wave functions has a node near $r = 1/2.\, R_o$ and in the interval $(0,\ 1/2.\, R_o)$ the contribution to the overlap is small, due to the presence of a d-state, the main contribution comes from the interval $(1/2.\, R_o, R_o)$. Therefore the largest matrix elements $F_{ll'}$ are those, whose optical model wave functions have a node approximately at $r = R_o$. For a purely real optical model potential this happens in our case for the angular momenta l = 0, 3 and 4; thus we expect that the important matrix elements $F_{ll'}$ are those with either l or l' equal to these values. The presence of the imaginary part of the potential does not alter this conclusion at our energy.

In fig. 7 the exact curve N. 2 is compared with the curve N. 2 A, which has been computed putting $F_{ll'} = 0$ unless either l or l' are equal to 0, 3 or 4 and not larger than 5. It is apparent that this selection of angular momenta does not change the qualitative features of the angular distribution, nor changes essentially the integral cross section. We can also proceed along the same lines for the Born approximation (curve N. 11). In the absence of any potential the overlap integrals are more sensitive to the small difference in the relative momenta in the two channels and the selection needs no more to be symmetri

cal in l and l'. For example, the amplitude F_{20} is expected to be important, while F_{02} is expected to be small. The other important terms are those with either l or l' equal to 1, 2 or 3 and not larger than 3. The effect of this selection of angular momenta in the Born approximation is shown in fig. 7 (curve N. 11B) and it is apparent that it does not change significantly the angular distribution.

We have thus shown that the optical model distortion operates a selection of angular momenta, which is different from that one in the Born approximation. We can also show that the optical model selection itself is sufficient to account for the qualitative change in the most important linear momentum transfer as compared with that expected in the Born approximation: in fact, using the selection of angular momenta appropriate to the distorted wave Born approximation, but the amplitudes $F_{ll'}$ calculated in the Born approximation, we get the curve 11A plotted in fig. 8, which clearly shows a maximum at the smallest allowed value of the linear momentum transfer, as curve N. 2 does. On the contrary, the Born approximation selection of angular momenta is not sufficient to give, with the amplitudes $F_{ll'}$ calculated in the distorted wave approximation, an angular distribution resembling curve N. 11 (see curve N. 2B in fig. 8). This is to be expected, because the optical model distortions differently modify the relative amplitudes and phases of the relevant amplitudes $F_{ll'}$, as compared with those of the Born approximation. In particular, this happens in presence of resonance effects: these, in our example, enhance the amplitude of the scattering states inside the potential well for the angular momentum quantum numbers l = 2 and 4 in the neutron channel and l' = 1 in the proton channel.

We emphasize that these remarks on the relation between linear and angular momentum transfer with and without optical model distortions are in a sense complementary to those of Austern, Butler and Pearson[25].

With regard to the agreement with the experimental data, we have found[26] that it is definitely improved by taking into account exchange in the effective finite-range n-p interaction. Details on this and related results will be reported and discussed in a forth-coming paper.

REFERENCES.

(1) - H. E. Gove, Proc. Rutherford Jubilee Int. Conf. (Heywood and Co. Ltd, London, 1961).

(2) - Proc. of the Int. Symposium on direct interactions, Padua 1962 (to be published).

(3) - W. Tobocman, Theory of direct nuclear reactions (Oxford Univ. Press, 1961).

(4) - L. Colli, M. G. Marcazzan, F. Merzari, P. G. Sona and P. Tomaš, Nuovo Cimento 20, 928 (1961).

(5) - C. H. Townes, Handbuch der Physik 38/1, edited by S. Flügge (Springer Verlag, Berlin 1958).

(6) - L. Colli, I. Iori, S. Micheletti and M. Pignanelli, Nuovo Cimento 21, 966 (1961).

(7) - C. Bloch, Nuclear Physics 4, 503 (1957).

(8) - G. E. Brown, Rev. Mod. Phys. 31, 839 (1959).

(9) - A. Agodi and E. Eberle, Nuovo Cimento 18, 718 (1960).

(10) - L. Rosenfeld, Nuclear Physics 26, 594 (1961).

(11) - M. E. Rose, Elementary theory of angular momentum (Wiley, New York 1957).

(12) - H. Feshbach, Ann. Rev. Nucl. Sc. 8, 49 (1958).

(13) - N. F. Mott and H. S. Massey, Theory of atomic collisions (Oxford Univ. Press, 1949).

(14) - M. H. Hull and G. Breit, Handbuch der Physik 41/1, edited by S. Flügge (Springer Verlag, Berlin, 1959).

(15) - E. U. Condon and G. H. Shortley, Theory of atomic spectra (Cambridge Univ. Press 1957).

(16) - G. Racah, Phys. Rev. 61, 186 (1942); ibidem 62, 438 (1942); ibidem 63, 367 (1943).

(17) - P. M. Endt and C. Van Der Leun, Nuclear Physics 34, 1 (1962).

(18) - T. Lamarsh and H. Feshbach, Phys. Rev. 104, 1633 (1956).

(19) - A. Agodi, R. Giordano, G. Schiffrer and M. Giannini, (to be published).

(20) - I. Talmi, Helv. Physica Acta 25, 185 (1952).

(21) - . Schrandt, J. R. Beyster, M. Walt and E. W. Salmi, LA Report 2099 (1957).

(22) - A. E. Glassgold, W. B. Cheston, M. L. Stein, S. B. Schuldt and G. W. Erikson, Phys. Rev. 106, 1207 (1957).

(23) - P. E. Hodgson and J. R. Rook, Nuclear Physics 37, 632 (1962).

(24) - D. H. Wilkinson, Proc. of the Int. Conf. on Nuclear Structure, Kingston (North-Holland, Amsterdam, 1960).

(25) - S. T. Butler, N. Austern and C. Pearson, Phys. Rev. 112, 1227 (1958).

(26) - A. Agodi, R. Giordano and G. Schiffrer, Physics Letters, 4, 253 (1963).

TABLE I

Set of parameters used for the angular distributions plotted in the figures.

Curve Number	R_o	V_n	V_p	W_n	W_p	η
1	5. 40	40	40. 4	8	9. 2	0. 646
2	4. 85					
3	4. 40					
4	4. 40	44				
5	4. 40		44. 4			
6	4. 40			8. 8		
7		30				
8			30			
9		30	30			
10	4. 85	0	0	0	0	
11	4. 85	0	0	0	0	0

Curves N. 1, 2 and 3 have been determined by the optical model parameters which fit the elastic scattering data for neutrons [21] and for protons [22]. Only the parameter values which have been varied with respect to those of curve N. 1 are indicated. The values of the other parameters are: $R_n = R_p = 4.40$; $a_n = 0.35$; $a_p = 0.19$.

We have assumed $R_{on} = R_{op} = R_o$. Lengths are measured in units of 10^{-13} cm, energies in MeV.

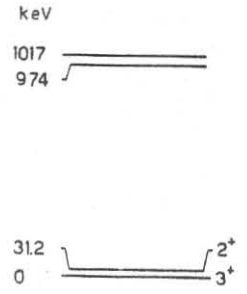

Fig. 1- Energy levels of the nucleus ^{28}Al (from ref. (17)).

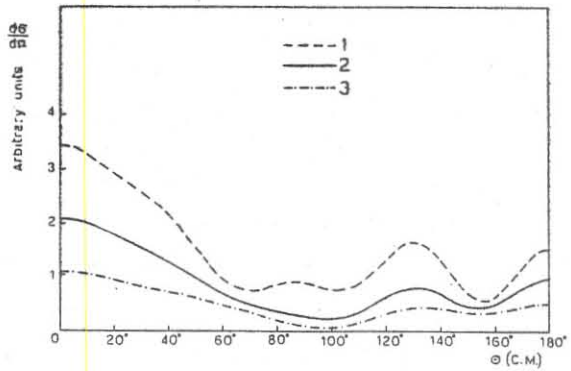

Fig. 2- Variation of the bound state parameter R_o. R_o = 5. 40 (N. 1); R_o = 4. 85 (N. 2); R_o = 4. 40 (N. 3) The curves in all figures are numbered according to table I.

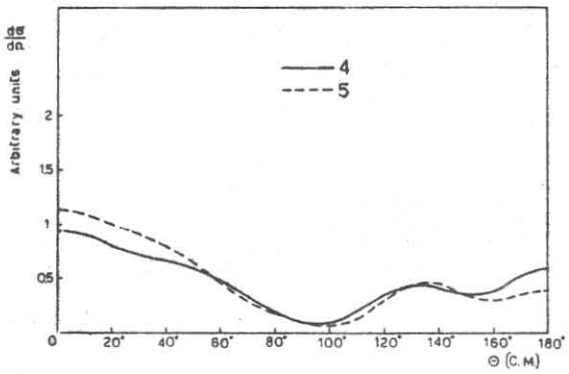

Fig. 3- Small variations in the real part of the optical potential. V_n = 44 MeV (N. 4); V_1 = 44. 4 MeV (N. 5).

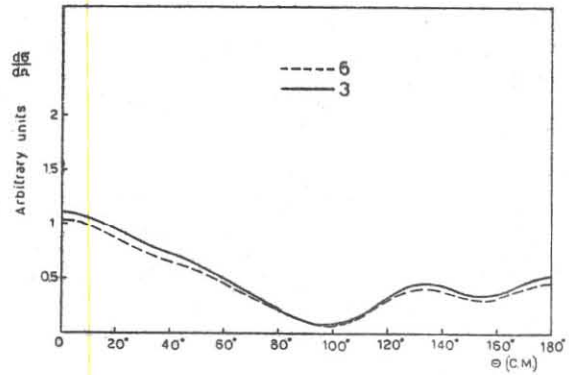

Fig. 4- Small variation in the imaginary part of the optical potential. W_n = 8. 8 MeV (N. 6); W_n = 8 MeV (N. 3).

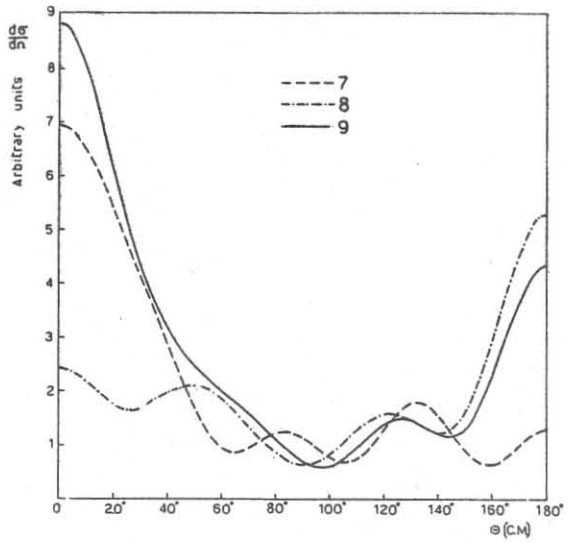

Fig. 5- Large variations in the real part of the optical potential. V_n = 30 MeV (N. 7); V_p = 30 MeV (N. 8); $V_n = V_p$ = 30 MeV (N. 9).

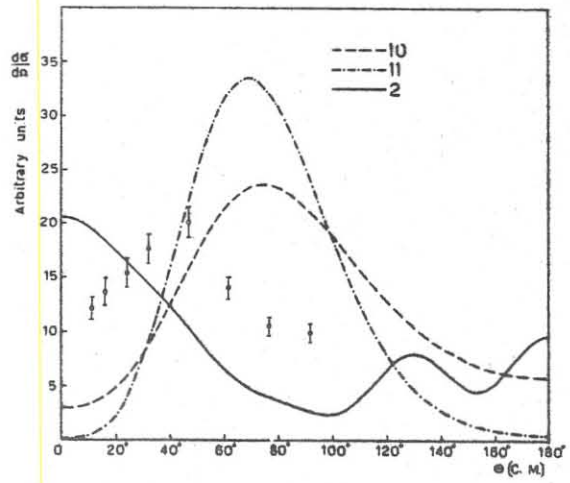

Fig. 6- Large variations in the optical potentials. Distorted waves Born approximation (N. 2); Coulomb distortion only (N. 10); no distortion (N. 11). Experimental points from ref. (4). Curve N. 2 has been multiplied by a factor 10.

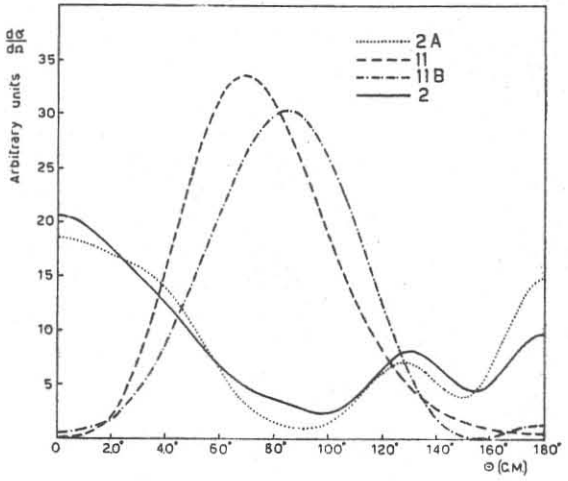

Fig. 7- Selection of important angular momenta. Curves N. 2A and N. 11B are defined in the text. Curves N. 2 and 2A have been multiplied by a factor 10.

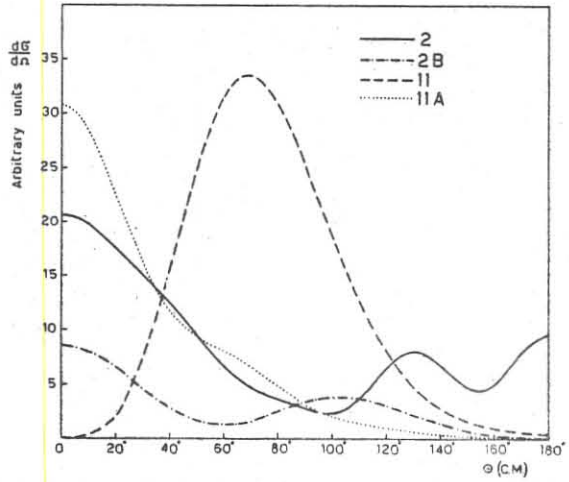

Fig. 8- Crossed selection of important angular momenta. Curves N. 2B and 11A are defined in the text. Curves N. 2 and 2B have been multiplied by a factor 10.